TU Delft

Delft University of Technology

Document Version
Final published version

Citation (APA)
Tang, J., & van Bussel, G. J. W. (2018). Wind tunnel testing airfoil with screens at low reynolds number. In *Wind Energy Symposium* Article AIAA 2018-0995 (Wind Energy Symposium, 2018). American Institute of Aeronautics and Astronautics Inc. (AIAA). https://doi.org/10.2514/6.2018-0995

Important note
To cite this publication, please use the final published version (if applicable).
Please check the document version above.

Copyright
In case the licence states “Dutch Copyright Act (Article 25fa)”, this publication was made available Green Open Access via the TU Delft Institutional Repository pursuant to Dutch Copyright Act (Article 25fa, the Taverne amendment). This provision does not affect copyright ownership.
Unless copyright is transferred by contract or statute, it remains with the copyright holder.

Sharing and reuse
Other than for strictly personal use, it is not permitted to download, forward or distribute the text or part of it, without the consent of the author(s) and/or copyright holder(s), unless the work is under an open content license such as Creative Commons.

Takedown policy
Please contact us and provide details if you believe this document breaches copyrights.
We will remove access to the work immediately and investigate your claim.

This work is downloaded from Delft University of Technology.

Green Open Access added to TU Delft Institutional Repository

'You share, we take care!' - Taverne project

https://www.openaccess.nl/en/you-share-we-take-care

Otherwise as indicated in the copyright section: the publisher is the copyright holder of this work and the author uses the Dutch legislation to make this work public.

AIAA SciTech Forum
8–12 January 2018, Kissimmee, Florida
2018 Wind Energy Symposium

10.2514/6.2018-0995

Check for updates

Wind Tunnel Testing Airfoil with Screens at Low Reynolds Number

Juan Tang[1] and Gerard J.W. van Bussel [2]
Delft University of Technology, Delft, 2629 HS, The Netherlands

It is well known that ducted wind turbine (DWT) captures more mass flow through the interior of the duct compared to the same size of bare wind turbine. The duct geometry is usually generated by airfoils shaped annular wings. To this end, a new high-lift airfoil for duct application is developed. This paper describes the wind tunnel testing methodology that has been applied to determine the two-dimensional characteristic of an airfoil for a Reynolds number of 1.0 × 10^5. A particular aspect of the experiments is the presence of a screen, simulating the pressure drop over a real rotor. The experiments are performed in the 0.4 m × 0.4 m W-wind tunnel of the Delft University of Technology. The two-dimension model is composed of an airfoil and a uniform porous screen. Measurements are conducted with the varying angle of attack and wind speed. To investigate the effect of screen loading on the airfoil pressure distribution, three different screens, with thrust coefficient equals to 0.46, 0.65 and 1.06, respectively, are tested. Tests on the airfoil with screens show the lift coefficient increases compared to the pure airfoil configuration. For fixed angle of attack, the airfoil pressure difference does not linearly increases with the increasing screen loading. By coupling with different screen loading has different influence on the airfoil lift, combining with the screen has C_T = 0.46 achieves the highest C_l in the vicinity of angle of attack (4° ≤ α ≤ 15°), and coupling with the high screen loading (C_T = 0.65 and 1.06) at high angle of attack (α ≥ 20°) is also beneficial for the tested airfoil in terms of C_l. The results also show the combination with screen delays the stall angle.

Nomenclature

T	=	thrust
V_0	=	free stream velocity
A_s	=	screen area
C_T	=	thrust coefficient
Kvel	=	ratio of upstream velocity to velocity at model quarter-chord point
V_u	=	uncorrected free stream velocity
c	=	chord
h_{ts}	=	test section height
ε_{sb}	=	solid blockage
ε_{wb}	=	wake blockage
C_d	=	drag coefficient
C_{du}	=	uncorrected drag coefficient
C_l	=	lift coefficient
C_{lu}	=	uncorrected lift coefficient
Re	=	Reynolds number
α	=	angle of attack (degr.)

I. Introduction

LOW Reynolds number (Re) aerodynamics of airfoils apply to miscellaneous applications, such as model wind turbine rotor and wind turbines.[1,2] From the precedent literature, it appears that the S822 and S823 airfoils are

[1] PhD Candidate, Wind Energy Research Group, J.Tang-6@tudelft.nl, AIAA Member.
[2] Professor, Wind Energy Research Group, G.J.W.vanBussel@TUDelft.nl, AIAA Member.

Copyright © 2018 by the American Institute of Aeronautics and Astronautics, Inc. All rights reserved.

Downloaded by Technische Universiteit Delft on February 13, 2025 | http://arc.aiaa.org | DOI: 10.2514/6.2018-0995

the only two airfoils that have been specially designed for small horizontal axis wind turbine (HAWT) blades. These two airfoils are principally intended for stall-regulated HAWTs and form one of the nine advanced NREL airfoil families.[3] Later on, Giguere and Selig,[4] designed new airfoils for small variable-speed HAWT blades and tested at Reynolds number between 1×10^5 and 5×10^5. Timmer[5] conducted an airfoil test for VAWT to investigate the characteristics of the NACA 0018 airfoil for steady two-dimensional low Reynolds number operation.

Ducts are used to augment the power output and wind turbine rotors with ducts are known as ducted wind turbine (DWT) or diffuser augmented wind turbine (DAWT). The airfoil considered here is designed for an annular duct with high lift coefficients to achieve more airflow passing through the interior of the duct. Airfoils for such model ducts typically operate in the Reynolds number range 2×10^5 to 5×10^5. Consequently, there is a need for new design for airfoil shaped ducts for DWT. To supplement the limited data currently available for high lift airfoils at low Reynolds number, a new modified airfoil is tested over a range of Reynolds number between 0.8×10^5 to 1.6×10^5.

Accurate measurements of low Reynolds number airfoil performance using pressure taps is key to understand and improve the performance of low Reynolds number airfoils. Most aerodynamic performance measurement techniques for airfoils rely on using balance system or pressure system, or a combination of both. The approach described in this paper uses pressure taps to obtain lift and pressure drag data and the wake rake method to obtain drag. Sections II and III of this paper describe the experiment method. Section IV presents the results first, the pressure profiles on the pure airfoil and the airfoil with screens with varying angle of attack. Second, lift coefficient on the configuration of the airfoil with different screens as compared with pure airfoil. The paper ends with conclusions drawn from this research.

Downloaded by Technische Universiteit Delft on February 13, 2025 | http://arc.aiaa.org | DOI: 10.2514/6.2018-0995

II. Design Philosophy

The present airfoil is designed for an annular duct requiring high lift coefficients, instead of a high lift-to-drag ratio. Since high lift is the only desirable feature when modifying an airfoil for duct application, the factors most related to enhanced high-lift low Reynolds numbers airfoil performance are investigated. Previous experimental data of a three-dimension airfoil-shaped duct model are used as well. Combining these data, and applying a Liebeck type high-lift design philosophy, the thickness, the camber and the shape of leading and trailing edges are determined through the fully inversed method. The XFOIL 6.99 code is used as the analysis tool in this study.

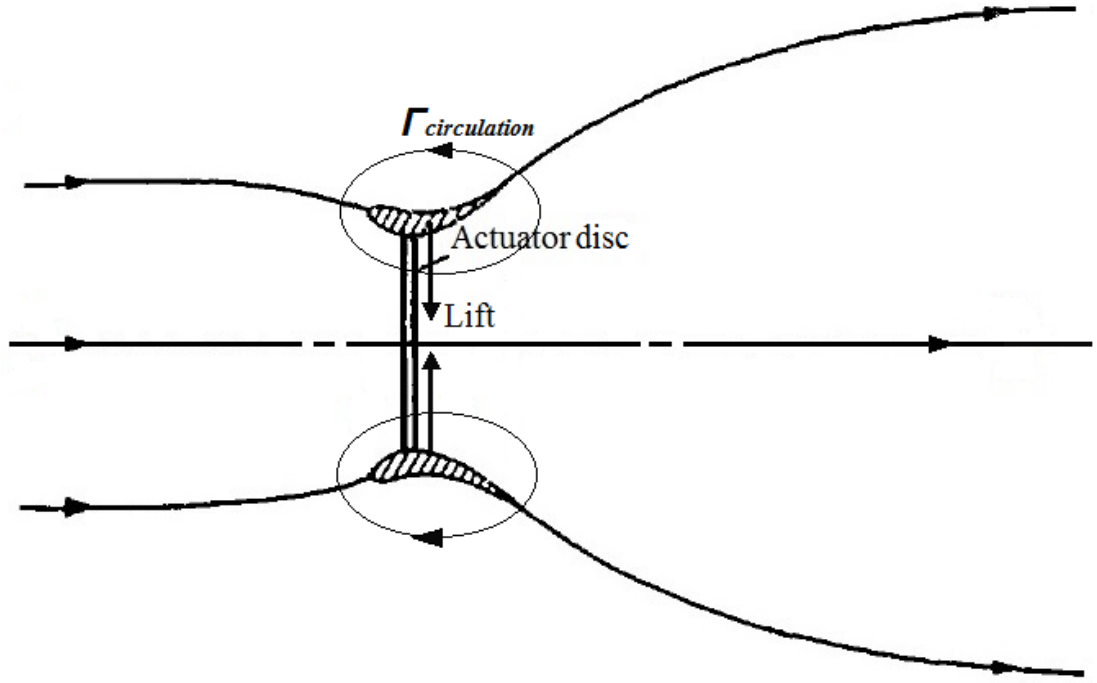


Fig. 1 Aerofoil-shaped duct with actuator disc (rotor simulator) in inviscid flow.[6]

With a specified velocity distribution, it is found that an increase of both camber and thickness of the duct leads to an enhancement in lift coefficient with the presence of the pressure drop generated by rotor. In particular, the thickness increment for the aft part of the airfoil generates higher lift coefficient. Also the fact that the airfoil should perform well in the presence of a screen (representing the pressure drop of the rotor in a complete D(A)WT design) has consequences for the design choice. Previous experimental data show that, with the screen presence, the front stagnation point moves towards the inner part of the duct. Consequently, the pressure coefficient reduces in the front part of the suction side, although the pressure differences, between the upper surface and the lower surface, of the duct fore part enlarges. Decreasing the leading edge radius, in essence, accelerates the airflow around it so that a negative area is created.

In the study of DWT, frequently the actuator disc assumption is used to model the turbine blades. In this model, the rotor is replaced by a uniform porous screen across which a pressure drop is explicitly imposed. This simplification makes it a useful tool during the preliminary design stage. It does not, however, capture potentially interesting aspects of the flow physics near the blade and in the wake of a DWT. In addition, the actuator disc model cannot predict the effect of the turbine wake on flow separation along the walls of the duct. This effect is negligible in this study as the investigation concentrates on the duct rather than rotor. The installation of screen divides the duct into two parts, the duct fore part starts from the leading edge until the screen plane, while the duct aft part includes the screen plane to trailing edge.

A high-lift airfoil based on the preceding discussion and presented in the following section is designed and manufactured. XFOIL is used for rapid interactive design: if a candidate airfoil failed to meet the design goals, the earlier experience is used to reanalyse and redesign the airfoil to more closely match the desired high-lift performance objectives. The iterative process continued until a successful airfoil is designed, and subsequently, wind tunnel tests are conducted to validate the design philosophy. It is expected this specially tailored airfoil for the duct should provide enhanced performance with the presence of screen.

III. Wind Tunnel Facility and Measurement Techniques

This section presents the wind tunnel experiments used to validate the design philosophy discussed in the previous section. A detailed description of two-dimensional airfoil model, the TU Delft low speed W-wind tunnel facilities, test section flow quality, and lift and drag measurement techniques are given in this section.

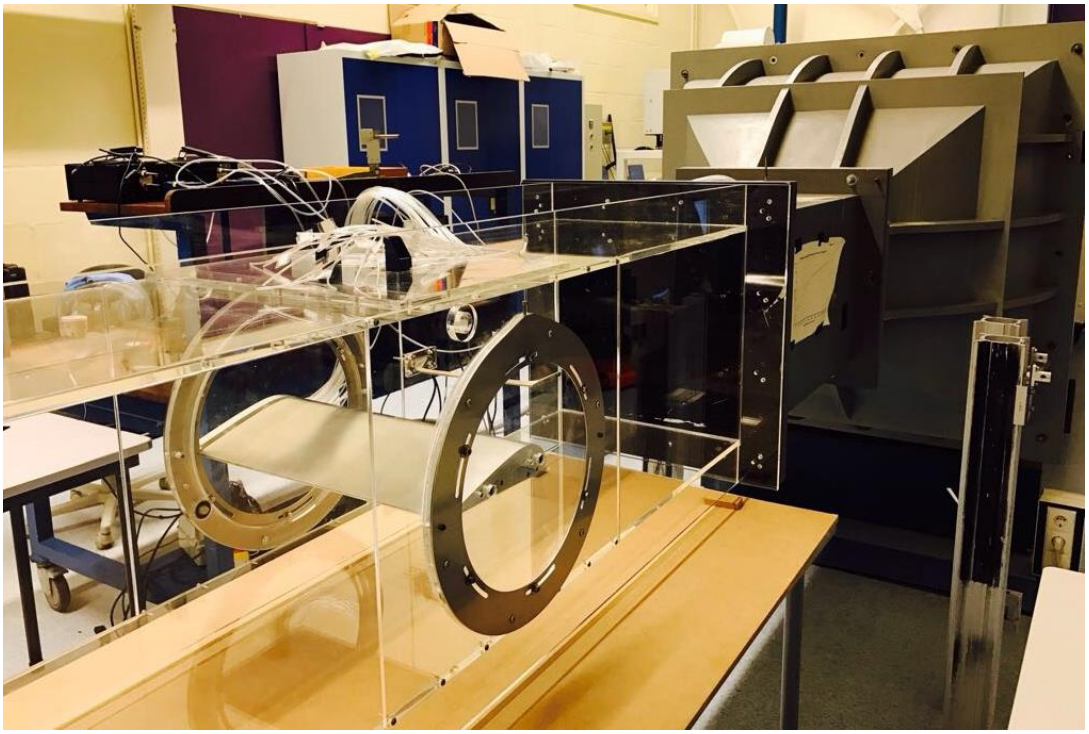


Fig. 2 Photograph of wind tunnel test section with the pure airfoil model present.

Downloaded by Technische Universiteit Delft on February 13, 2025 | http://arc.aiaa.org | DOI: 10.2514/6.2018-0995

Downloaded by Technische Universiteit Delft on February 13, 2025 | http://arc.aiaa.org | DOI: 10.2514/6.2018-0995

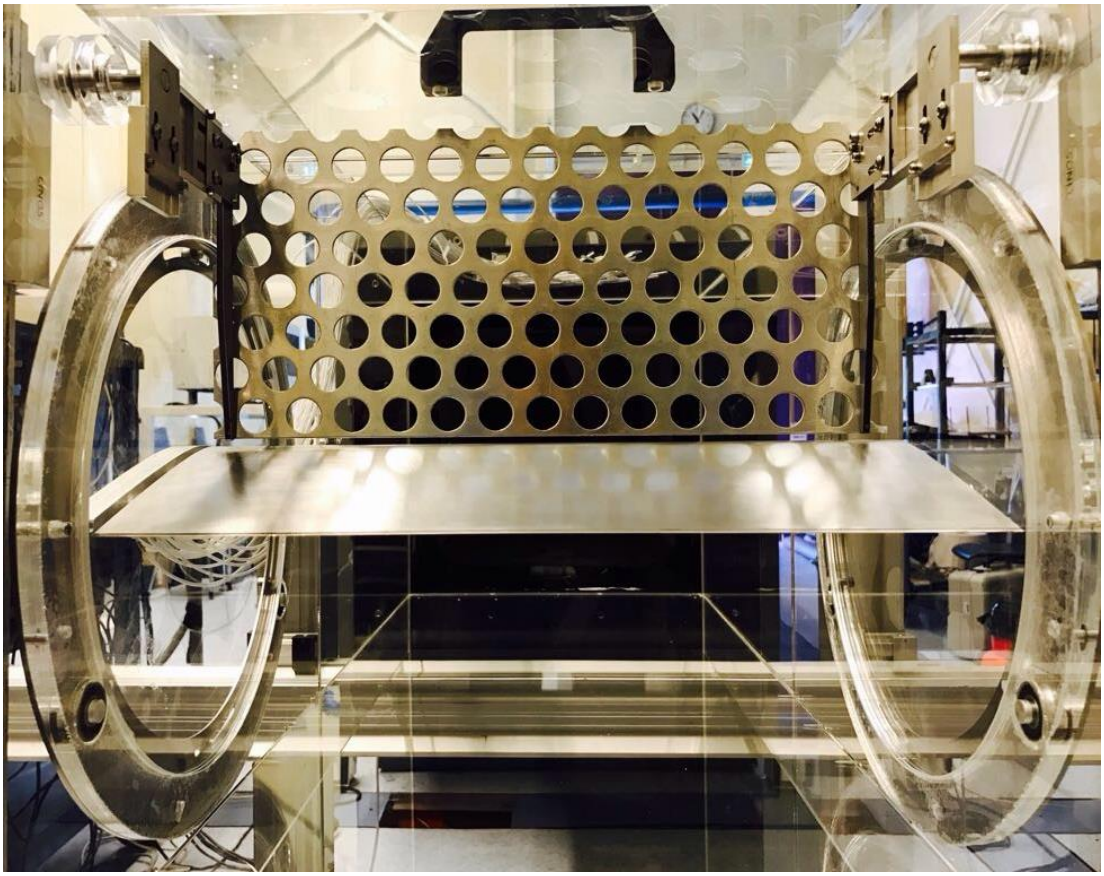


Fig. 3 Airfoil model setup with a porous screen.

A. Wind tunnel description

The experimental setup is depicted in Fig. 2 and Fig. 3. The low Reynolds number airfoil measurements described here are conducted in the W-tunnel of TU Delft. The wind tunnel is an open-circuit low-speed wind tunnel with a test section of 0.4 m × 0.4 m × 1.5 m. The maximum free-stream velocity in the test-section is 35 m/s. To ensure good flow quality in the test section, the tunnel settling chamber contains a thick honeycomb and anti-turbulence screens, resulting in a turbulence level less than 0.5% over the Reynolds number range tested. For a nominal test-section speed of 7.6 m/s, a Reynolds number of 1.0×10^5 based on an airfoil chord of 0.2 m is realized.

In order to change the angle of attack, the test section has two mechanically coupled rotary plates flush mounted in the (detachable) side walls, as can be seen in Fig. 2. This design is chosen to conveniently mount the model horizontally with the centre of rotation in the middle of the test section length. The centre of rotation for the model has been set at 25% of the chord length from the leading edge. The free-stream dynamic pressure is determined from a pitot probe in the settling chamber.

Tests are performed at Reynolds number varying from 0.8×10^5 to 1.6×10^5. The data are taken over the airfoil angle of attack range from 0˚ to 20˚, with steps of 5˚. Measurements are taken at static positions of each angle of attack, using an integration time of 30 s for each angle of attack measured. Pressure are acquired using digital temperature compensated ESP scanners with ranges adapted to the maximum readings, being 5 psi for wake rake and wall, and 15 or 45 psi for the airfoil, depending on the dynamic pressure level. To gain necessary accuracy in the high pressured environment all pressures are measured against a tunnel reference pressure, which reads a value of the free-stream static pressure.

B. Airfoil Model and Screen model

The basic airfoil is a modification of Donqi airfoil which is designed by a Dutch commercial company. It has a maximum relative thickness of 14% at the x/c = 30%. The camber is 6.09% at the x/c = 55%. Compared with original airfoil, the maximum of relative thickness value and its location, as well as the camber have been changed respectively to reveal the influence of thickness and camber have on the performance of airfoil in low Reynolds number.

For the current tests, the 0.2 m chord and 0,4 m span airfoil model is mounted horizontally, covering the entire span of the test section width. For clarity, the model has cylindrical connections which are clamped to the rotary plate on the test section side walls. The model also is equipped with a levelling plate to set the zero angle of attack.

The lift is calculated by integrating the pressure distribution over the airfoil. For this purpose all the models are instrumented with 0.4 mm diameter pressure taps. The model static pressures and the wake rake static and total pressures are fed to an electronic pressure scanner system. Data are recorded using an electronic data acquisition system and are on line processed using the laboratory computer.

As shown in Fig. 3, the model is composed of a numerically milled aluminium airfoil and a uniform porous screen. The experimental setup is based on the assumption that a two dimensional duct flow is symmetrical, thus only half part of the setup is realised. The top wall of the wind tunnel is the plane of symmetry and hence represents the centreline of a two dimensional duct. The screen is always positioned at the airfoil chord wise position closest to the upper wall of the test section i.e. in the "nozzle" of the set up. The axial force on the screen T, across which a pressure drop is explicitly imposed, is expressed by the thrust coefficient C_T, according to equation (1).

$$C_T = \frac{T}{\frac{1}{2}\rho v_0^2 A_S} \tag{1}$$

Where ρ is the fluid density, v_0 is free-stream velocity and As is the screen area. The thrust coefficients of the screens experienced in this study are C_T = 0.46, 0.65, and 1.06 respectively.

The instrumentation of the test model consists of 30 pressure taps distributed along the chord of the airfoil and a wake rake with 40 total and 10 static pressure probes installed downstream of the airfoil. Airfoil drag is calculated from the flow loss of momentum by integrating the total and static pressures in the wake. Wake pressures are measured by a wake rake located 3.5 chords (700 mm) downstream of the trailing edge of the model. The wake rake is positioned vertically and at 200 mm from the centre line of the test section, in order to avoid possible interference caused by the model pressure taps. Tests are performed for angles of attack α ranging from 0° to 20°, in steps of 5°. At high angles of attack, the wake is so wide that the wake rake used during testing cannot capture the full wake extent. In this case, the pressure distribution on the model surface is integrated to obtain the drag. At high angles of attack, this pressure drag is predominant, hence it is acceptable to calculate the total drag with only the pressure drag.

C. Wind Tunnel Boundary Corrections

The presence of the wind tunnel walls increases the measured lift, and drag because of the increase in velocity perceived at the model. More specifically, the lateral walls in a two-dimensional testing context cause four phenomena: buoyancy, solid blockage ε_{sb}, wake blockage ε_{wb}, and streamline curvature.[7]

Buoyancy: Buoyancy is an additional drag force that results from a decrease in static pressure along the test section due to the growth of the boundary layer at the walls. Although buoyancy effects are usually insignificant even for airfoils tested within test sections having a constant area, the main effect of buoyancy is taken into account directly in corrections of the freestream velocity.

Solid Blockage: The physical presence of a model within a test section is known as solid blockage, which produces a decrease in the effective area. From the continuity and Bernoulli equations, the velocity of the air must increase as it flows over the model, increasing all aerodynamic forces and moments at a given angle of attack. The effect is greater at a given value of the ratio for the closed test section than for the open jet. Solid blockage is a function of the model size and test section dimensions.

Wake Blockage: It arises from a velocity within the airfoil wake that is lower than the freestream velocity. For closed test sections, in order to satisfy the continuity equation, the velocity at the model (outside of the wake) must increase. Wake blockage is frequently considered negligible with an open test section as the flow is free to expand. The effect of wake blockage is proportional to the wake size and thus to the measured drag on the model.

Streamline Curvature: Due to the physical constraints of the tunnel boundaries, the normal curvature of the free air as it passes over a lifting body (such as an airfoil) is changed, increasing the airfoil effective camber as the streamlines are “squeezed” together. For closed wind-tunnel sections, the increase in camber results in an increase in lift, pitching moment about the quarter-chord point, and angle of attack, while these parameters decrease in an open jet. The drag is unaffected by streamline curvature.

The velocity is also corrected to account for the boundary layer growth along the tunnel walls, which results in a slightly higher than free-stream velocity at the location of the model. By using a second velocity measuring probe at

Downloaded by Technische Universiteit Delft on February 13, 2025 | http://arc.aiaa.org | DOI: 10.2514/6.2018-0995

the model quarter-chord point with the model removed and then measuring the upstream and downstream velocities simultaneously over a wide range in the Reynolds number, a calibration curve is obtained. Thus, for a measured upstream velocity, the actual velocity at the model can be calculated. The resulting velocity correction curve used to account for boundary-layer growth is given by the equation (2)[7], where K_{vel} is ratio of free stream velocity to velocity at model quarter-chord point, and V_u is uncorrected free stream velocity.

$$K_{vel} = 1.015755 - 0.0002391 V_u + 0.00001712\sqrt{V_u} + \frac{0.1296}{\sqrt{V_u}} \tag{2}$$

The measured quantities that must be corrected can be sub-divided into two categories: stream and model quantities. The most important stream quantity is the velocity at the model. This velocity is obtained from the free-stream velocity measurements and by applying the proper corrections to account for solid and wake blockage as well as boundary-layer growth. Combining the velocity corrections in a single expression gives equation (3),

$$V_c = V_u K_{vel}(1 + \varepsilon_{sb} + \varepsilon_{wb}) \tag{3}$$

Other free-stream quantities, such as Reynolds number and dynamic pressure, are obtained directly from the corrected value of the velocity. The model quantities of interest are the lift, drag and angle of attack, which are corrected in their non-dimensional form to account for solid and wake blockage as well as streamline curvature. It is important to note that the use of drag data is required to correct the model quantities since wake blockage is proportional to the measured drag coefficient.

When the individual effects promoted by the interference between the walls and the airfoil, and the screen are known, the total alteration in the flow at the airfoil is found by superposition. The characteristics of the airfoil in the altered field of flow are compared with the characteristics in free air. The method of superposition, which is fundamental to the entire analysis, is in general inapplicable to compressible flow as the differential equation for such flow is nonlinear in the physical plane. The separate solutions are superposed by assuming the induced velocities are small as compared with the velocity of the undisturbed flow. Since the current experiments are conducted in low Reynolds number, namely, superposition of velocities is, in this case, technically permissible. Furthermore, the tunnel-wall corrections are in most cases rather small relative to the experimental quantities being corrected, so that it is not thought that the use of this approximate method will lead to large errors in the final corrected quantities. All the results presented in the next section are corrected.

IV. Results and discussion

This section provides an overview of the data obtained from the wind-tunnel tests conducted with the manufactured airfoil and the screen. The tested data set for a Reynolds number range of 0.8×10^5 - 1.6×10^5, though this Reynolds number range might not cover the entire operational range of DWT. As stated in the description of the experimental setup, free-stream velocities from 5 m/s to 10 m/s are investigated during the experiments. Only minor differences are found between these cases. Therefore, for the sake of conciseness, comparison between two-dimension airfoil data and the previous three-dimension data is reported only for V_0 = 7 m/s, corresponds to $Re = 1.0 \times 10^5$.

A. Pressure profile

Comparisons of pressure distribution between the pure airfoil and airfoil with screens for a Reynolds number of 1.0×10^5 are shown in Fig. 4 - Fig. 8.

Downloaded by Technische Universiteit Delft on February 13, 2025 | http://arc.aiaa.org | DOI: 10.2514/6.2018-0995

Downloaded by Technische Universiteit Delft on February 13, 2025 | http://arc.aiaa.org | DOI: 10.2514/6.2018-0995

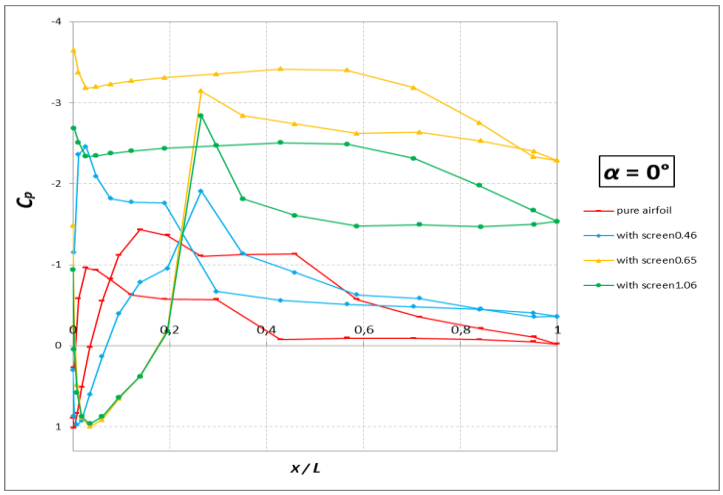


Fig. 4 Comparison between pure airfoil and airfoil with different screens at α = 0°.

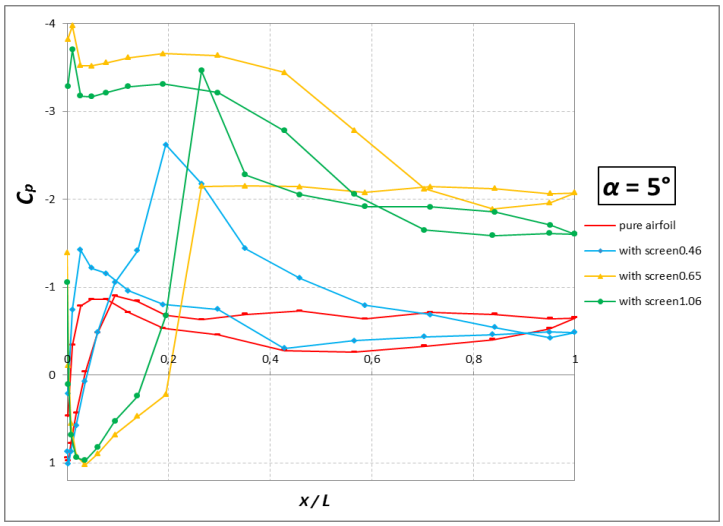


Fig. 5 Comparison between pure airfoil and airfoil with different screens at α = 5°.

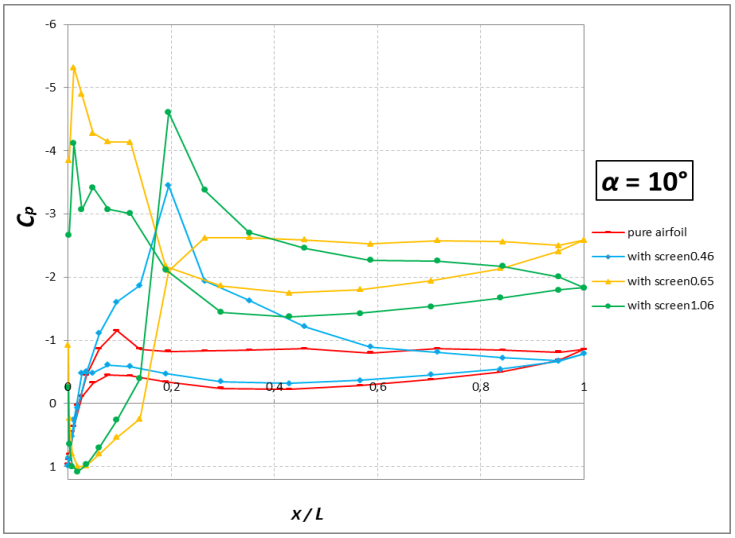


Fig. 6 Comparison between pure airfoil and airfoil with different screens at α = 10°.

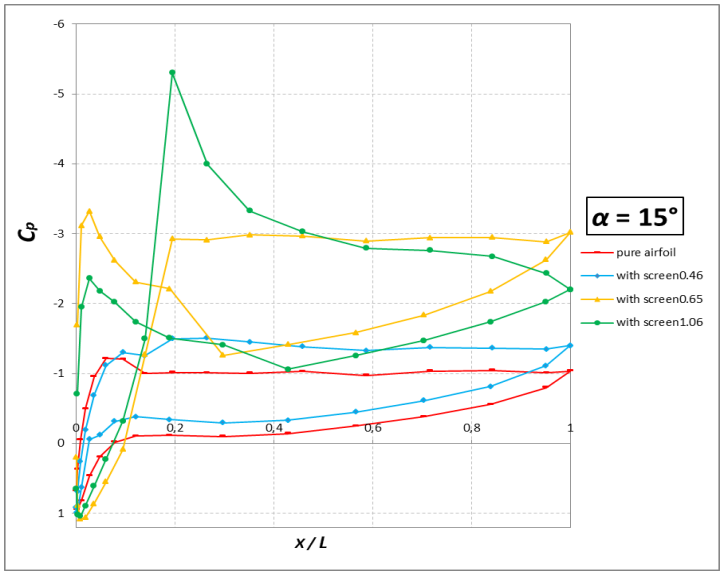


Fig. 7 Comparison between pure airfoil and airfoil with different screens at α = 15°.

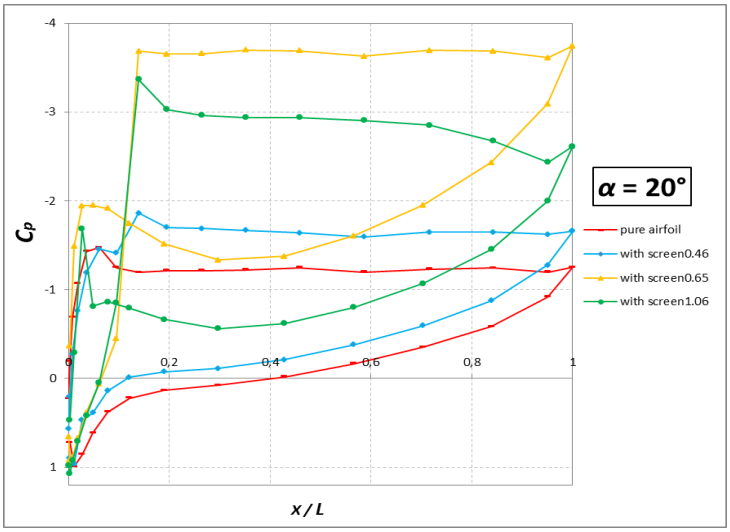


Fig. 8 Comparison between pure airfoil and airfoil with different screens at α = 20°.

In absence of the screen, the pressure profile of this thick airfoil is characterised by a stagnation point located on the suction side of the airfoil. The pressure difference between upper surface and lower surface decreases first ($\alpha \leq 5°$) then increases again with increasing angle of attack ($5° \leq \alpha \leq 20°$). Overall, the pressure distributions of pure airfoil in Fig. 6 - Fig. 8 report its poor performance as anticipated, and point out the presence of undesired velocity distribution that could lead to flow separation.

It is apparent to see the pressure drop on the airfoil upper surface caused by screen at $X/L = 0.2$ in Fig. 4 - Fig. 8. Focusing on Fig. 4 and Fig. 5, and more precisely on the airfoil fore part (area between leading edge and screen plane), it can be observed that the stagnation point moves backward by increasing the screen loading to 0.65 and 1.06, which agrees with the previous three-dimensional test results. This is because the decreased mass flow blocked by the high resistance of screen (high C_T), as the well-known axial momentum theory, the mass flow rate swallowed by a bare wind turbine is a decreasing function of turbine thrust coefficient. It is also noted that when the stagnation point moves towards to the screen plane, the acceleration flow around the leading edge reduces and thus the magnitude of pressure coefficient. Continuing on the airfoil fore part, by adding the screen, the pressure difference between the upper surface and lower surface enlarges. The higher the C_T, the larger the pressure difference is, this is also due to the effect of the screen resistance so that a huge acceleration has to take place to go around the pressure side.

Downloaded by Technische Universiteit Delft on February 13, 2025 | http://arc.aiaa.org | DOI: 10.2514/6.2018-0995

As the angle of attack increases ($\alpha \geq 10°$), the stagnation point moves forward again. At the same time the pressure difference in the airfoil fore part reduces, but grows in the airfoil aft part (area between the screen plane and trailing edge). It is easy to realize that the most important contribution to lift is the one due to the pressure differences generated by the airfoil aft part, when the airfoil coupled with screen, in particular high screen C_T. Moreover, the more and more flat negative pressure profile of the suction side suggest the occurrence of separation.

Considering the tip clearance, the gap between the screen and the airfoil suction side, which generates the acceleration flow attached to the airfoil suction side, therefore contributes to the lower pressure coefficient compared to the pure airfoil. The higher the C_T, the more resistance it creates thus pushing more air pass through the tip clearance to have the acceleration, which is beneficial to suppress or delay the flow separation.

Now turning to the airfoil aft part near to the trailing edge, there is a slight velocity increase for both configurations of pure airfoil and airfoil with screens when the angle of attack is greater than 10°. It occurs to pure airfoil at angle of attack of 10°, while for airfoil with higher screen C_T, this velocity acceleration takes place with higher angle of attack. The reason may be that the tiny air bubbles sticking to the upper surface disturb the flow, and the disorder following transition interferes with the records.

To summarize, the influence of the thrust coefficient on the airfoil pressure distribution at different angles of attack is visibly reported in Fig. 4 - Fig. 8. The presence of screen on the airfoil suction side steepens its pressure gradient, then it maintains at a "high" level and is weakened owing to the inverse pressure gradient till the trailing edge. It effectively leads to a pressure differences and therefore increases the lift. For fixed angle of attack, the airfoil pressure difference does not linearly increases with the increasing C_T. The high screen loading (C_T = 0.65 and 1.06) at high angle of attack ($10° \leq \alpha \leq 20°$) is more beneficial for the tested airfoil. Among the three screens, the screen with C_T =0.65 achieves the best performance for tested angle of attack. In totality, the tested airfoil shows good performance combined with screens, in spite of the possibility of separation presence at high angle of attack.

B. Lift Data

Comparison of lift coefficient for $Re = 1.0 \times 10^5$ between pure airfoil and airfoil with screens against the angle of attack in Fig. 9.

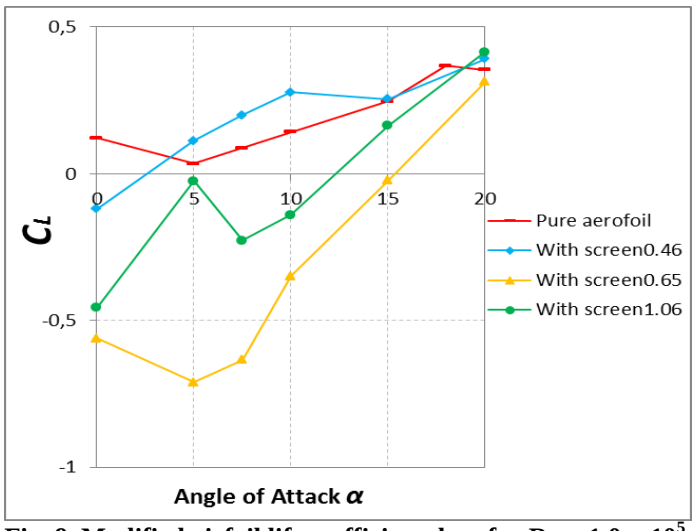


Fig. 9 Modified airfoil lift coefficient data for Re = 1.0 × 10^5.

As seen in Fig. 9, the tested airfoil for duct is, not like typical of those found for low Reynolds number airfoil flows in which the lift curve linearly increases with angle of attack, insensitive to the low angle of attack ($0° \leq \alpha \leq 5°$). The C_l plot of the airfoil with the screens indicates that, coupling with different screen loading has different influence on the airfoil lift. By coupling with low screen loading (C_T = 0.46), the airfoil obtains lift increment for angle of attack ($4° \leq \alpha \leq 15°$), then it nearly coincides with the pure airfoil lift for higher angle of attack ($\alpha \geq 15°$). It is seen that adding the high loading screen (C_T = 0.65 and 1.06) impairs the lift coefficient for the tested airfoil. However, based on the slope, it can be deduced that for angle of attack ($\alpha \geq 19°$), the C_l of airfoil with screen will be greater than the C_l of pure airfoil, both for the low loading and the high loading. In particular, the airfoil with the screen has C_T = 0.46 obtains the highest C_l in the vicinity of angle of attack ($4° \leq \alpha \leq 15°$). It implies that the tested airfoil for duct is suitable for low screen loading for specific angle of attack, or high screen loading at high angle of attack. It is also

Downloaded by Technische Universiteit Delft on February 13, 2025 | http://arc.aiaa.org | DOI: 10.2514/6.2018-0995

inferred that compared to normal low Reynolds number airfoil, the tested airfoil with screen delays the stall angle, since C_l keep increasing until the angle of attack reaches 20°.

V. Conclusion

In this paper, the effect of screen loading on an airfoil for duct has been experimentally analyzed by means of a two-dimensional model. In particular, great efforts are addressed to the discrepancies between the pure airfoil and the airfoil loaded with a screen, which is particularly difficult to be predicted without known data. For this reason a simplified two-dimensional model has been applied, the model consists of an airfoil and a uniform porous screen fixed at the suction side of the airfoil. Three screens with a thrust coefficient (C_T) equals to 0.46, 0.65 and 1.06, respectively have been tested.

In comparison to other low Reynolds number airfoil available in the literature, the tested airfoil shows unsatisfying performance with itself. However, results have shown that the combination of screen has beneficial effect onto the airfoil aerodynamic performance. In more detail, it is found that increasing the screen loading (C_T) the stagnation point moves towards the screen plane at low angle of attack ($0° \leq \alpha \leq 10°$), then moves forward to leading edge again when keep increasing angle of attack ($10° \leq \alpha \leq 20°$). This phenomenon is determined by the effect of high screen loading so that less mass flow is passed through the screen.

It has also shown that, by adding the screen, the pressure difference between the upper surface and lower surface enlarges. The higher the C_T, the larger the pressure difference is at the airfoil fore part, this is due to the effect of the screen resistance so that a huge acceleration has to take place to go around the pressure side. Furthermore, the pressure plots display that the most important contribution to lift is due to the pressure differences generated by the airfoil aft part, when the airfoil is coupled with the screen, in particular with high screen C_T. However, the flat pressure profile of the suction side suggests the occurrence of separation.

The slight velocity increment near the trailing edge is noticeable for both configurations of the pure airfoil and the airfoil with screens. It occurs to the pure airfoil at angle of attack of 10°, while for airfoil with higher screen C_T, this velocity acceleration takes place with higher angle of attack. The reason may be that the tiny air bubbles sticking to the upper surface disturb the flow, and the disorder following transition interferes with the records.

For fixed angle of attack, the airfoil pressure difference does not linearly increases with the increasing C_T. By coupling with different screen loading has different influence on the airfoil lift, combining with the screen has C_T = 0.46 achieves the highest C_l in the vicinity of angle of attack ($4° \leq \alpha \leq 15°$), and coupling with the high screen loading (C_T = 0.65 and 1.06) at high angle of attack ($\alpha \geq 20°$) is also beneficial for the tested airfoil.

To summarize, the presence of screen on the airfoil suction side steepens its pressure gradient, then it maintains at a high negative level and is weakened owing to the adverse pressure gradient till the trailing edge. It effectively leads to a pressure differences and therefore increases the lift. Moreover, the presence of screen delays the flow separation owing to the tip clearance effect. In totality, analysis indicate that aerodynamic characteristics of the tested airfoil has enhanced performance, especially combined with high screen loading, in spite of the possibility of separation presence at high angle of attack.

Acknowledgments

Financial support provided by the STW organization (grant number-12728) from the Netherlands and the CSC Scholarship from the Chinese government is gratefully acknowledged.

References

[1] Giguere, P., and M.S. Selig, "Aerodynamic Performance of Small Wind Turbines Operating at Low Reynolds Numbers," *American Wind Energy Association WIND POWER '96 Conference,* Denver, CO: 1996.

[2] Giguere, P., and Selig, M. S., "Low Reynolds Number Airfoils for Small Horizontal Axis Wind Turbines," *WIND ENGINEERING*, vol. 21, 1997, pp. 367 – 380.

[3] Tangier, J. L., and Somers, D. M., *NREL Airfoil Families for HAWTs*, Washington, DC: 1995.

[4] Giguère, P., and Selig, M. S., "New Airfoils for Small Horizontal Axis Wind Turbines," *Journal of Solar Energy Engineering*, vol. 120, 1998, p. 108.

[5] Timmer, W. A., "Two-dimensional low-Reynolds number wind tunnel results for airfoil NACA 0018," *Wind ENGINEERING*, vol. 32, 2008, pp. 525–537.

[6] De Vries, O., *Fluid Dynamic Aspects of Wind Energy Conversion*, 1979.

[7] Barlow, J. B., Rae, W. H., and Pope, A., *Low-Speed Wind Tunnel Testing*, New York: John Wiley & Sons, 1999.

Downloaded by Technische Universiteit Delft on February 13, 2025 | http://arc.aiaa.org | DOI: 10.2514/6.2018-0995